

Tuning the initial phase to control the final state of a driven qubit: single-passage coherent destruction of tunneling

Polina O. Kofman,^{1,2,3,4,*} Sergey N. Shevchenko,¹ Franco Nori^{3,5,6}

¹*B. Verkin Institute for Low Temperature Physics and Engineering, Kharkiv 61103, Ukraine*

²*V. N. Karazin Kharkiv National University, Kharkiv 61022, Ukraine*

³*Theoretical Quantum Physics Laboratory, Cluster for Pioneering Research, RIKEN, Wakoshi, Saitama 351-0198, Japan*

⁴*University of Lisbon and Instituto de Telecomunicações, Avenida Rovisco Pais 1, Lisboa, 1049-001 Portugal*

⁵*Quantum Computing Center, RIKEN, Wakoshi, Saitama 351-0198, Japan*

⁶*Department of Physics, The University of Michigan, Ann Arbor, MI 48109-1040, USA*

(Dated: August 8, 2023)

A driven quantum system can experience Landau-Zener-Stückelberg-Majorana (LZSM) transitions between its states, when the respective energy levels quasi-cross. If this quasicrossing is passed repeatedly under periodic driving, the trajectories can interfere either constructively or destructively. In the latter case, known as coherent destruction of tunneling, the transition between the energy states is suppressed. Even for a *double*-passage case, the accumulated phase difference (also referred to as the Stückelberg phase) can lead to destructive interference, resulting in no transition. In this paper we discuss a similar process for a *single*-passage dynamics. We study the LZSM single-passage problem starting from a superposition state. The phase difference of this initial state results in interference. When this is destructive, resulting in a zero transition probability, such situation can be called *single-passage coherent destruction of tunneling*. When the phase is chosen so that the occupation probabilities do not change after the transition, this can be called *occupation conservation* and this is analogous to the problem of *transitionless driving*. We demonstrate how varying the system parameters (driving velocity, initial phase, initial detuning) can be used for quantum control.

I. INTRODUCTION

For quantum computing it is important to have different methods on how to steer quantum systems to desired states, see e.g. Refs. [1–4]. The ability to predict the behavior of the system opens the opportunity to use it either as a quantum logic gate or to improve already existing gates. Which means to make the process faster or the errors smaller, or easier for an experimental realization.

A dynamics that allows the system to return to its *original* state can be useful for quantum information. This can be realized by means of adiabatically slow driving [5–9]. We could also consider the following question: is it possible to return to the original state using fast processes? In some cases this is possible [10, 11]. A large number of parameters exist by which we can drive the system. If the signal is periodic, there are special values of the frequency and amplitude which guide the system to its ground state [12–16]. Since this appears as a result of destructive interference [17–22], is known as coherent destruction of tunneling (CDT).

In a different context, the problem of controlling a quantum system can be formulated as how to correct a given drive so that the system remained in one of the basis states. Such transitionless driving was studied in Ref. [23]; first for a generic case, and also for the particular situation of a two-level system with linear drive.

This last case corresponds to Landau-Zener-Stückelberg-Majorana (LZSM) transitions [24–27]. LZSM transitions are interesting in different aspects and processes, including: axion-photon conversion [28], interferometry in a non-Hermitian N -body interacting boson system [29], interference effects of a qubit [30–34], Mach-Zehnder-type interferometry in a superconducting qubit [35, 36], tunneling under the effect of higher-order dispersion [37], spin-flip in the multi-stage Stern–Gerlach experiment [38]. LZSM transitions can be driven with intense laser pulses in the avoided-crossing band structure of graphene’s Dirac cones [39–42]; different transition scenarios were demonstrated, including limiting cases such as CDT and the intermediate case of occupation preservation.

Here we study similar questions to the ones in Refs. [13, 23]: how to steer the system to a given state? Can we stay in the same state as before the driving (also known as *transitionless driving*)? What is needed to direct and guide the system to its ground state (also known as CDT)?

In our case, we consider the simplest linear driving and starting from a generic superposition state, using the initial phase difference between the spinor components as a *tunable parameter*. In our approach, considering the phase as a controlling parameter, we follow Ref. [43]. What we mean is illustrated in Fig. 1, showing the dynamics of a qubit, when starting from three different superposition states, with the same initial occupation probability but with three different phase differences between the spinor components. The three respective curves show (from bottom to top): coherent destruction of tunneling

* polinaokofman@gmail.com

(CDT, bottom), remaining at the same position as the initial one (middle), and obtaining maximal occupation probability (constructive interference, opposite to CDT) shown in the top curve. In general, *changing the initial phase gives the possibility to obtain any probability between constructive and destructive ones.*

The rest of the paper is organized as follows. In Section II we describe the dynamics and introduce important aspects of the adiabatic-impulse approximation (with details of the adiabatic stage of the dynamics in Appendix A). In Section III we find the dependence of the final probability on the system's parameters, including the initial phase. In Section IV we analyze the range of the possible values of the final occupation probability. The eventual return of the system to its initial state and single-passage CDT are discussed in Section V. In Section VI we describe how to control the qubit only by changing its phase and linear perturbations. The respective results in the adiabatic basis are presented in Appendix C. In Appendix D, we generalize the result for any type of dynamics which could be described by the adiabatic impulse model.

II. DYNAMICS: ADIABATIC-IMPULSE APPROXIMATION

Consider the dynamics of a two-level system with a linear perturbation. Such a system is described by the Schrödinger equation

$$i\hbar \frac{\partial}{\partial t} |\psi\rangle = -\frac{1}{2} (\Delta \sigma_x + \varepsilon(t) \sigma_z) |\psi\rangle, \quad (1)$$

where

$$\varepsilon(t) = vt, \quad (2)$$

Δ and v are constant values and σ_i stands for the Pauli matrices. Such dynamics describe the Landau-Zener-Stückelberg-Majorana (LZSM) transitions, with the excitation probability (see Ref. [25] and references therein)

$$\mathcal{P} = \exp(-2\pi\delta), \quad (3)$$

(if starting from the ground state), where

$$\delta = \Delta^2 / (4v\hbar) \quad (4)$$

is the adiabaticity parameter.

The dynamics with initial time t_i and final time t_f can be described by the adiabatic-impulse approximation [44]. The dynamics could be separated into three different stages [21]: adiabatic evolution, transition, and adiabatic evolution again:

$$|\psi_f\rangle = U_{\text{ad}}(t_f, 0) N U_{\text{ad}}(0, t_i) |\psi_i\rangle, \quad (5)$$

where $|\psi_{i,f}\rangle$ are the initial and final wave functions, U_{ad} describes the adiabatic evolution, and N describes the

LZSM transition. The adiabatic-evolution matrix before the transition is

$$U_{\text{ad}}(0, t_i) = \begin{pmatrix} \exp(-i\zeta) & 0 \\ 0 & \exp(i\zeta) \end{pmatrix}, \quad (6)$$

and after the transition the adiabatic-evolution matrix is

$$U_{\text{ad}}(t_f, 0) = \begin{pmatrix} \exp(i\zeta) & 0 \\ 0 & \exp(-i\zeta) \end{pmatrix}. \quad (7)$$

Here the phase ζ and its asymptotic expressions at large times, i.e. at

$$t = \pm \tau_a \sqrt{\frac{2\hbar}{v}} \quad (8)$$

with $\tau_a \gg 1$, are the following [44]:

$$\zeta(\pm \tau_a) = \frac{1}{2\hbar} \int_0^{\pm \tau_a} \sqrt{\Delta^2 + 2\hbar v \tau^2} d\tau \approx \quad (9)$$

$$\approx \pm \left[\frac{\tau_a^2}{2} + \frac{\delta}{2} - \frac{\delta}{2} \ln \delta + \delta \ln \sqrt{2} \tau_a \right]. \quad (10)$$

A non-adiabatic transition is described by the transfer matrix N , which is associated with a scattering matrix in scattering theory [45]. The components of the transfer matrix are related to the amplitudes of the respective states of the system in energy space. The diagonal elements of N [24, 25] correspond to the square root of the reflection coefficient R , and the off-diagonal elements correspond to the square root of the transmission coefficient T and its complex conjugate:

$$N = \begin{pmatrix} \sqrt{R} & \sqrt{T} \\ -(\sqrt{T})^* & \sqrt{R} \end{pmatrix}. \quad (11)$$

In our problem, these elements are

$$R = \mathcal{P} \quad \text{and} \quad T = (1 - \mathcal{P}) \exp(i2\varphi_S), \quad (12)$$

where φ_S is the Stokes phase

$$\varphi_S = \frac{\pi}{4} + \text{Arg}[\Gamma(1 - i\delta)] + \delta(\ln \delta - 1). \quad (13)$$

In what follows we will use the formalism summarized in this section (and explained at length in Refs. [24, 44]) to describe the system dynamics when starting from a superposition state. Note that Γ denotes the Gamma special function. Using these results it is possible to describe not only a single passage but also the multiple-passages case using the adiabatic-impulse model approximation.

III. DEPENDENCE OF THE FINAL STATE ON THE INITIAL PHASE

Consider the dependence of the final occupation probability on the initial phase of the wave function. For this, we take the wave function in the form

$$|\psi\rangle = \begin{pmatrix} \alpha \\ \beta \end{pmatrix}. \quad (14)$$

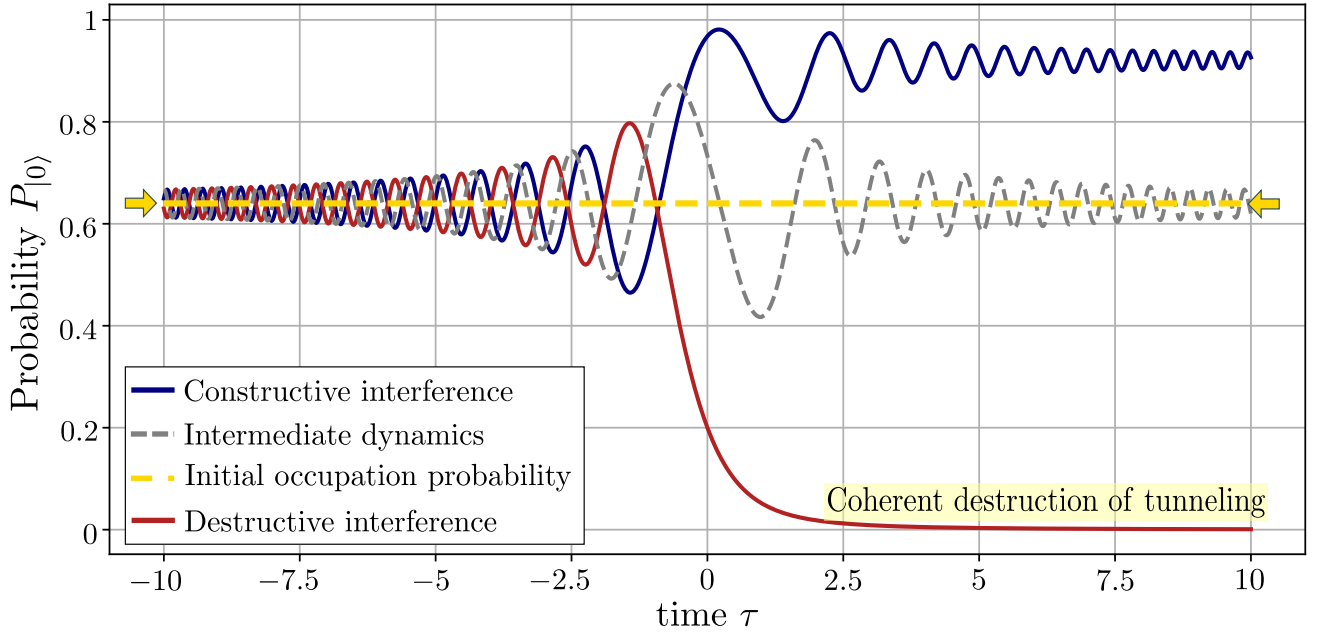


FIG. 1. Dependence of the occupation probability on the dimensionless time $\tau = \sqrt{v/(2\hbar)}t$. The three curves show three possible different occupation probabilities starting from the same initial occupation probability $P_{|0\rangle}$ and *different initial phases* of the wave function. The maximum value of the occupation probability $P_{|0\rangle}$ corresponds to constructive interference (dark blue curve). The phase in this case is defined in Eq. (23) and approximately equals to $\phi_i \approx 0.36$. The minimal value of the occupation probability corresponds to destructive interference (dark red curve). The phase, in this case, is defined in Eq. (22) and approximately equals to $\phi_i \approx 1.53$. Any occupation probability between these values, defined by the constructive and destructive interferences, could be obtained by changing the initial phase. In particular, there are parameters which allow the system to return to its initial state (grey dashed curve). The adiabaticity parameter must correspond to the condition defined in Eq. (31) and then the initial phase is equal to the value in Eq. (32) (in the plot above this approximately equals to $\phi_i \approx -2.78$).

Then taking α_i real for the initial condition, we introduce the phase difference in β_i :

$$\beta_i = \sqrt{1 - \alpha_i^2} \exp(i\phi_i). \quad (15)$$

The *single*-passage evolution is described by the Hermitian matrix

$$\tilde{N} = U_{\text{ad}}(\tau_f, 0) N U_{\text{ad}}(0, \tau_i). \quad (16)$$

Taking for simplicity $\tau_f = \tau_a$ and $\tau_i = -\tau_a$, we obtain the components of this matrix

$$\begin{pmatrix} \tilde{N}_{11} & \tilde{N}_{12} \\ \tilde{N}_{21} & \tilde{N}_{22} \end{pmatrix} = \begin{pmatrix} \sqrt{R} & \sqrt{T}e^{2i\zeta(\tau_a)} \\ -\sqrt{T}^*e^{-2i\zeta(\tau_a)} & \sqrt{R} \end{pmatrix}. \quad (17)$$

For a more general case, $\tau_f \neq -\tau_i$, see Appendix A. The wave function after the transition can be derived from Eq. (5). Then the first component of the spinor becomes

$$\alpha_f = \alpha_i \tilde{N}_{11} + \sqrt{1 - \alpha_i^2} e^{i\phi_i} \tilde{N}_{12}. \quad (18)$$

The final occupation probability of the lower level is $|\alpha_f|^2 = P_{|0\rangle_f}$. Then using Eqs. (10,13), we can write the

direct dependence of the occupation probability on the system parameters

$$P_{|0\rangle_f} = \alpha_i^2 e^{-2\pi\delta} + (1 - \alpha_i^2)(1 - e^{-2\pi\delta}) + 2\alpha_i \sqrt{1 - \alpha_i^2} e^{-\pi\delta} \sqrt{1 - e^{-2\pi\delta}} \cos \theta, \quad (19)$$

where

$$\theta(\delta, \tau_a, \phi_i) = \frac{\pi}{4} + \text{Arg}[\Gamma(1 - i\delta)] + \tau_a^2 + 2\delta \ln(\sqrt{2}\tau_a) + \phi_i. \quad (20)$$

It is important to note that the final occupation probability does not depend on the final time; for details see Appendix A. The final result will be the same as Eq. (19), with $-\tau_a \rightarrow \tau_i$.

IV. HOW THE INITIAL PARAMETERS AFFECT THE FINAL PROBABILITIES

The final probability $P_{|0\rangle}$ depends on the following parameters: δ , α_i , ϕ_i , τ_i . We are now interested in studying the contribution of the third term in Eq. (19). This term is the result of interference, and (for convenience) we will

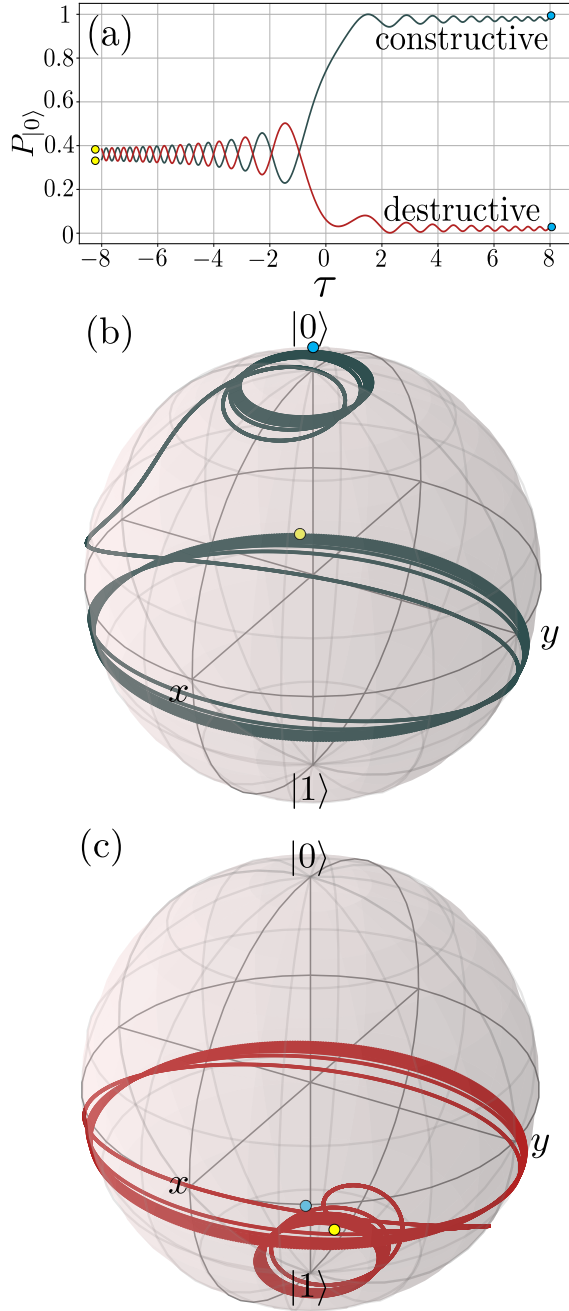


FIG. 2. Impact of the initial phase ϕ_i on the final occupation probability $P_{|0\rangle}$. If the value of the interference term in Eq. (21), is maximum, the final occupation probability is also maximum and corresponds to the constructive interference case. On the other hand, if (21) is minimal the final occupation probability $P_{|0\rangle}$ is also minimal, and this corresponds to the destructive interference case shown in panel (a). (b) shows the dynamics on the Bloch sphere for the *constructive* interference case shown in panel (a). (c) shows the dynamics on the Bloch sphere for the *destructive* interference case shown in panel (a). The initial occupation probability is $P_{|0\rangle i} = 0.36$ and the adiabaticity parameter is $\delta = \ln 2/2\pi$.

designate it as α_{int}^2

$$\alpha_{\text{int}}^2 = 2\alpha_i \sqrt{1 - \alpha_i^2} e^{-\pi\delta} \sqrt{1 - e^{-2\pi\delta}} \cos \theta. \quad (21)$$

Figure 2 shows the contribution of this interference term. If the initial probability is fixed and the phase difference between the components of the wave function is varied, we can obtain the final probabilities in a wide range.

The dependence on α_i is proportional to the factor $2\alpha_i \sqrt{1 - \alpha_i^2}$, so there is a maximum at $\alpha_i = 1/\sqrt{2}$.

The dependence on τ_i and ϕ_i is via the argument of $\cos \theta$. Since the parameters ϕ_i and τ_i both contribute to the final result only by entering in θ in Eq. (19), then their contribution is analogous.

The phase before the transition is the sum of the initial phase ϕ_i and the phase which was collected during the adiabatic evolution before the transition. The adiabatic evolution phase is associated with the initial time. Depending on this, there are minimum and maximum values of this interference term, which correspond to $\cos \theta = \pm 1$. The maximal value is the constructive interference case. The minimal value is the destructive interference case. These respective cases will occur if the initial phase shift is

$$\phi_i^{\text{destr}} = \phi_{i0} + \frac{\pi}{2}, \quad (22)$$

and

$$\phi_i^{\text{constr}} = \phi_{i0} - \frac{\pi}{2}, \quad (23)$$

where ϕ_{i0} corresponds to the zero contribution from the interference and equals to

$$\phi_{i0} = 2\pi n + \frac{\pi}{4} - \text{Arg} [\Gamma(1 - i\delta)] - \tau_i^2 - 2\delta \ln(\sqrt{2}\tau_i), \quad (24)$$

with n being an integer.

We can obtain any value of the interference term between the constructive- and destructive-interference values. The minimum and maximum values of the occupation probability are

$$P_{|0\rangle \text{max/min}} = \left(\alpha_i e^{-\pi\delta} \pm \sqrt{1 - \alpha_i^2} \sqrt{1 - e^{-2\pi\delta}} \right)^2. \quad (25)$$

The width of this region (between destructive and constructive interference) is

$$\Delta P(\alpha_i, \delta) = 4\alpha_i \sqrt{1 - \alpha_i^2} e^{-\pi\delta} \sqrt{1 - e^{-2\pi\delta}}. \quad (26)$$

The maximum value of the width, at $\alpha_i = \frac{1}{\sqrt{2}}$, is

$$\Delta P(\delta)_{\text{max}} = 2e^{-\pi\delta} \sqrt{1 - e^{-2\pi\delta}}. \quad (27)$$

Alternatively, the width could be changed by the adiabaticity parameter δ . In particular, if $\delta = \ln \sqrt{2}/\pi$, then the width becomes

$$\Delta P(\alpha_i)_{\text{max}} = 2\alpha_i \sqrt{1 - \alpha_i^2}. \quad (28)$$

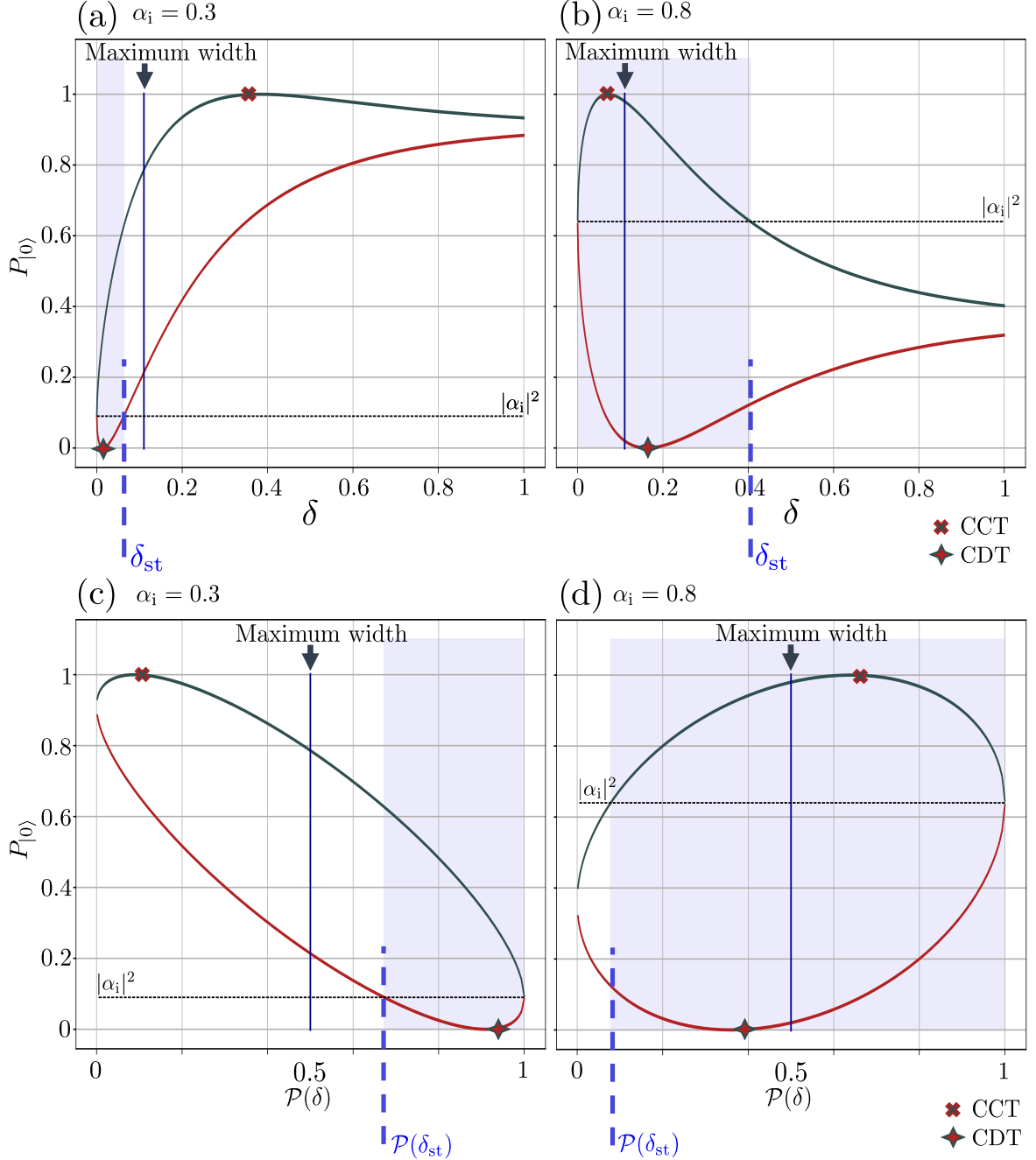


FIG. 3. Visualization of the difference (or width) between constructive and destructive interference in the dependence of the occupation probability on the adiabaticity parameter δ [upper panels] and on the single-passage probability $\mathcal{P}(\delta)$ [lower panels]. (a) and (c) correspond to the case when $\alpha_i = 0.3$, while (b) and (d) are for $\alpha_i = 0.8$. The dark green curve shows the constructive case, and the dark red curve shows the destructive interference case. The light blue background region shows the values of the adiabaticity parameter where conserving the occupation probability is possible, that is when $\delta < \delta_{st}$. The point which corresponds to the coherent destruction of tunneling (CDT) is indicated by a star and the coherent construction of tunneling (CCT) point is marked by an X-cross. The values of the adiabaticity parameter in these cases correspond to Eqs. (33, 34) respectively.

If we take

$$\alpha_i = \frac{1}{\sqrt{2}} \quad \text{and} \quad \delta = \frac{\ln \sqrt{2}}{\pi} \quad (29)$$

at the same time, the width will be 1, which means that the final probability could be obtained.

Figure 3 shows the dependence of the width between constructive and destructive interference on the adia-

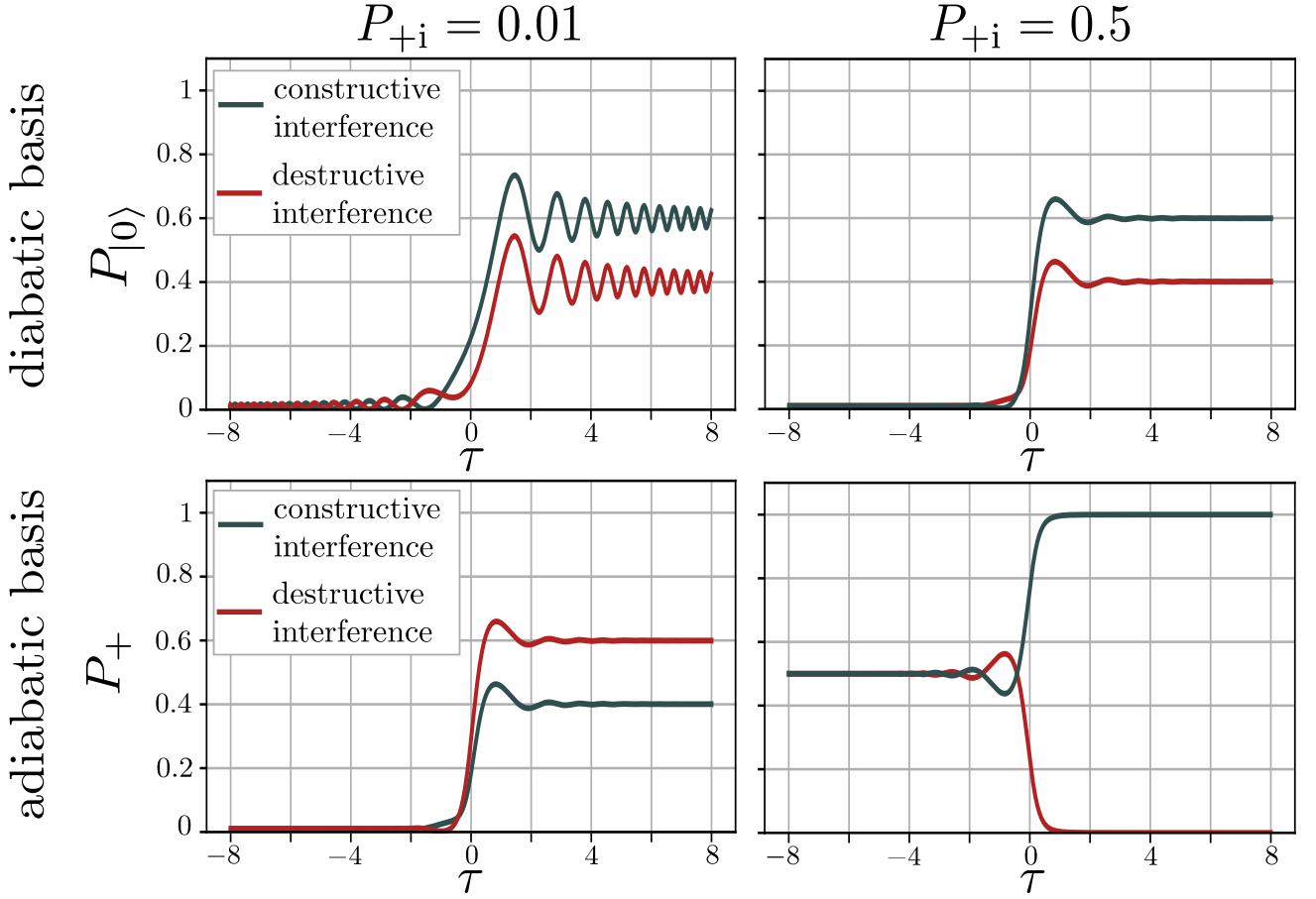


FIG. 4. Multiple-passage dynamics. The first row plots show the dynamics for *two* passages on a *diabatic* basis. The left column plots show the dynamics of the *single* LZSM transition with $\delta = \frac{\ln \sqrt{2}}{\pi}$ starting with an initial occupation probability $P_{|0\rangle_i} = 0.01$. The final states are between the dark green curve (constructive interference) and the dark red curve (destructive interference). The right column shows the *second* passage with the same as the first δ starting from one of the possible final stages after one transition. After the second transition, the final occupation probability could be chosen between 0 and 1 using as a tunable parameter the phase of the wave function before the second transition. The same dynamics is shown in the second row.

baticity parameter δ as well as on the single-passage probability $\mathcal{P}(\delta)$ in two cases of the initial occupation probability. The dark green line shows the maximal value of Eq. (21) and the dark red line the minimal value. The impact of the interference term depends on the adiabaticity parameter. When $\delta \gg 1$ and $\delta \ll 1$, the impact of the interference term tends to zero. Values of the adiabaticity parameters, when the interference impact is not negligible, correspond to the fast processes which are not adiabatic.

V. RETURNING TO THE INITIAL STATE AFTER THE TRANSITION

The condition for returning to the same state as the initial one after the transition could be found from Eq. (19) if we require $P_{|0\rangle} = \alpha_i^2$, which determines the value of

$\cos \theta$:

$$\cos \theta = \frac{(2\alpha_i^2 - 1) \sqrt{1 - \exp(-2\pi\delta)}}{2\alpha_i \sqrt{1 - \alpha_i^2} \exp(-\pi\delta)}. \quad (30)$$

This condition can be satisfied when the value of $|\cos \theta| \leq 1$, which requires

$$\delta \leq \delta_{\text{st}} = \frac{1}{2\pi} \ln \frac{1}{(2\alpha_i^2 - 1)} = -\frac{1}{2\pi} \ln (2\alpha_i^2 - 1). \quad (31)$$

Then the phase difference between α_i and β_i should be

$$\phi_i = \arccos \frac{(2\alpha_i^2 - 1) \sqrt{1 - e^{-2\pi\delta}}}{2\alpha_i \sqrt{1 - \alpha_i^2} e^{-\pi\delta}} + \phi_{i0} - \frac{\pi}{2}. \quad (32)$$

In Fig. 3 the region where there could be conservation of the initial occupation probability is shown as a light blue region. In the *diabatic* basis, it corresponds mostly to the small values of the adiabaticity parameter δ . Small δ corresponds to fast processes.

As noticed in the introduction, obtaining the ground state is important for quantum calculations. In Fig. 3 we indicate the points when it is possible to obtain the system in the ground state. If the final occupation probability is equal to zero that means that the final state is equal to $|1\rangle$. This corresponds to the CDT case. In the opposite case, if the final occupation probability is equal to one, the state is $|0\rangle$. By analogy, we call this case the Coherent Construction of Tunneling (CCT).

These cases are present for any initial occupation probability and correspond to the minimum and maximum of the destructive and constructive interference occupation probabilities. From Eq. (25) the values of the adiabaticity parameter for these cases could be found

$$\delta_{\text{CDT}} = -\frac{1}{2\pi} \ln(1 - \alpha_i^2), \quad (33)$$

$$\delta_{\text{CCT}} = -\frac{1}{\pi} \ln \alpha_i. \quad (34)$$

The results of this section could be surprising because these indicate that, *it is possible for the occupation probability to return to its initial value by only using phase control*. CDT and CCT for single passage with linear drive exist for any initial occupation probability.

VI. PREPARING A DESIRED TARGET STATE BY ONLY CHANGING ITS INITIAL PHASE

We now consider *how to control qubits by changing their initial phase*. We consider a qubit undergoing adiabatic evolution. Now we consider the constant drive

$$\varepsilon(t) = \text{const} = \varepsilon_0 \quad (35)$$

in Eq. (1). If we apply a constant drive, the evolution of the wave function consists in changing the phase. In the Bloch sphere, this corresponds to a rotation around the z axis. The phase which will appear after this evolution during the time t_{wait} is

$$\phi_{\text{ad}} = \pm 2 \frac{\sqrt{\Delta^2 + \varepsilon_0^2}}{2\hbar} t_{\text{wait}}. \quad (36)$$

The sign of the phase depends on the sign of the drive ε_0 , see details in Appendix B. This means that using this type of signal we can change the phase of the wave function without changing the occupation probability. We can use it to control the phase to prepare the desired initial state before the LZSM transition.

As was discussed in the previous section, for any initial occupation probability $P_{|0\rangle}$ it is possible to obtain ground states. This means that by changing the adiabaticity parameter δ and the initial phase ϕ_i it is possible to obtain any desired final state.

If the initial state is close to the ground state, an infinite adiabaticity parameter δ is needed to obtain another

ground state. To overcome this difficulty we apply multiple passages. Thus, two or more LZSM transitions allow to obtain the final occupation probability with experimentally realizable parameters.

For illustration, Fig. 4 demonstrates two passages (in the diabatic basis see the first row panels). The first passage starts with an initial occupation probability $P_{|0\rangle i} = 0.01$. This state is close to the ground state $|1\rangle$. After the first LZSM transition (left panel) with the adiabaticity parameter $\delta = \ln \sqrt{2}/\pi$ the final occupation probability could be $P_{|0\rangle f} \approx 0.5 \pm 0.1$. Applying a second LZSM transition with the same adiabaticity parameter as one of the possible final states after the first transition, the final occupation probability is now spread in the range between 0 and 1. Thus, changing the phase of the wave function after the first transition allows the possibility to choose the final state after the next transition.

This process can be reconsidered in the adiabatic basis which is the eigen-energy levels basis. All these formulas could be obtained by the relation between diabatic and adiabatic basis; see details in Appendix C. The example of the double passage in the adiabatic basis is shown in the second row in Fig. 4.

After the single LZSM passage, any final state could be obtained using as the tunable parameters the initial phase and adiabaticity parameter. The multi-passage dynamics with finite adiabaticity parameters could be applied in cases when obtaining some final stages of the infinite adiabaticity parameter is required for the single passage case.

VII. CONCLUSIONS

We analyzed the single passage qubit dynamics with a linear drive $\varepsilon(t) = vt$. The initial phase of the wave function was considered as a parameter. Several results (such as recovering the initial occupation probability, CDT, and CCT) were derived; these are summarized in Table I. We obtained target occupation probabilities using phase control. Also, multiple passages were considered to obtain desired qubit states for a given value of the adiabaticity parameter. Results are shown in Table I.

ACKNOWLEDGMENTS

The authors acknowledge fruitful discussions with Oleg Ivakhnenko. The research work of P.O.K. and S.N.S. is sponsored by the Army Research Office under Grant No. W911NF-20-1-0261. P.O.K. gratefully acknowledges an IPA RIKEN scholarship. F.N. is supported in part by: Nippon Telegraph and Telephone Corporation (NTT) Research, the Japan Science and Technology Agency (JST) [via the Quantum Leap Flagship Program (Q-LEAP)], and the Moonshot R&D Grant Number JP-MJMS2061], the Asian Office of Aerospace Research and

Type of the dynamics	Initial phase φ_i and adiabaticity parameter δ	Final occupation probability $P_{ 0\rangle i}$
Zero interference impact	$\phi_{i0} = 2\pi n + \frac{\pi}{4} - \text{Arg}[\Gamma(1 - i\delta)]$ $-\tau_i^2 - 2\delta \ln(\sqrt{2}\tau_i)$	$\alpha_i^2 e^{-2\pi\delta} + (1 - \alpha_i^2)(1 - e^{-2\pi\delta})$
Destructive interference	$\phi_i^{\text{destr}} = \phi_{i0} + \frac{\pi}{2}$	$\left(\alpha_i e^{-\pi\delta} - \sqrt{1 - \alpha_i^2} \sqrt{1 - e^{-2\pi\delta}}\right)^2$
Constructive interference	$\phi_i^{\text{constr}} = \phi_{i0} - \frac{\pi}{2}$	$\left(\alpha_i e^{-\pi\delta} + \sqrt{1 - \alpha_i^2} \sqrt{1 - e^{-2\pi\delta}}\right)^2$
Returning to initial occupation probability	$\phi_i = \arccos \frac{(2\alpha_i^2 - 1)\sqrt{1 - e^{-2\pi\delta}}}{2\alpha_i \sqrt{1 - \alpha_i^2} e^{-\pi\delta}} + \phi_{i0} - \frac{\pi}{2}$ and $\delta \leq -\frac{1}{2\pi} \ln(2\alpha_i^2 - 1)$	Initial occupation probability $P_{ 0\rangle i}$
Coherent destruction of tunneling	$\phi_i = \phi_i^{\text{destr}}$ and $\delta_{\text{CDT}} = -\frac{1}{2\pi} \ln(1 - \alpha_i^2)$	0
Coherent construction of tunneling	$\phi_i = \phi_i^{\text{constr}}$ and $\delta_{\text{CCT}} = -\frac{1}{\pi} \ln \alpha_i$	1

TABLE I. Summary of the main results. If the adiabaticity parameter δ can have any value, we do not show it in the second column, like in the first three lines.

Development (AOARD) (via Grant No. FA2386-20-1-4069), and the Foundational Questions Institute Fund (FQXi) via Grant No. FQXi-IAF19-06.

Appendix A: Different initial and final times

The values of the initial and final times are not the same in the general case. In this section, we will show the generalization of the transfer matrix, Eq. (17). Different initial and final times correspond to the value of phase which will occur due to adiabatic evolution. We use the following notations for values of the initial and final times respectively τ_i, τ_f . Following Ref. [44] the adiabatic evolution matrix before the transition is

$$\tau < 0: U_{\text{ad}}(0, \tau_i) = \begin{pmatrix} \exp(-i\zeta(\tau_i)) & 0 \\ 0 & \exp(i\zeta(\tau_i)) \end{pmatrix} \quad (\text{A1})$$

and after it becomes

$$\tau > 0: U_{\text{ad}}(\tau_f, 0) = \begin{pmatrix} \exp(i\zeta(\tau_f)) & 0 \\ 0 & \exp(-i\zeta(\tau_f)) \end{pmatrix}. \quad (\text{A2})$$

Now we consider a bias which is linear in time $\varepsilon(t) = vt$. The asymptotic expressions for ζ at large times, i.e. at $t = \pm\tau_a \sqrt{2\hbar}/v$, with $\tau_a \gg 1$ defined at Eq. (10).

In general, Eq. (17) becomes

$$\tilde{N} = \begin{pmatrix} \exp(i\zeta(\tau_f) - i\zeta(\tau_i)) \sqrt{\mathcal{P}} & \exp(i\zeta(\tau_f) + i\zeta(\tau_i) + i2\varphi_S) \sqrt{1 - \mathcal{P}} \\ -\exp(-i\zeta(\tau_f) - i\zeta(\tau_i) - i2\varphi_S) \sqrt{1 - \mathcal{P}} & \exp(-i\zeta(\tau_f) + i\zeta(\tau_i)) \sqrt{\mathcal{P}} \end{pmatrix}. \quad (\text{A3})$$

The final components of the wave function then become

$$\alpha_f = \exp[i\zeta(\tau_f) - i\zeta(\tau_i)] \sqrt{\mathcal{P}} \alpha_i + \exp[i\zeta(\tau_f) + i\zeta(\tau_i) + i2\varphi_S + i\phi_i] \sqrt{1 - \mathcal{P}} \sqrt{1 - \alpha_i^2}, \quad (\text{A4})$$

$$\beta_f = -\exp[-i\zeta(\tau_f) - i\zeta(\tau_i) - i2\varphi_S] \sqrt{1 - \mathcal{P}} \alpha_i + \exp[-i\zeta(\tau_f) + i\zeta(\tau_i) + i\phi_i] \sqrt{\mathcal{P}} \sqrt{1 - \alpha_i^2}. \quad (\text{A5})$$

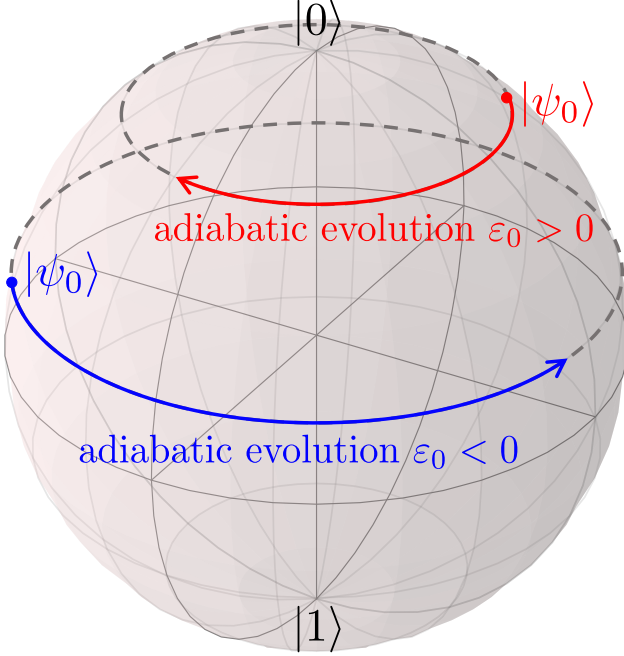


FIG. 5. Adiabatic evolution on the Bloch sphere. Two adiabatic evolutions are shown on the Bloch sphere. The red evolution shows that when the drive is constant and $\varepsilon_0 > 0$, the evolution corresponds to a clockwise (seeing from the top) rotation around the z -axis. If the drive is $\varepsilon_0 < 0$, the rotation turns counterclockwise. This case is shown in blue.

This gives the final state depending on the initial phase difference between the spinor components. It is important when we want to describe the dynamics with multiple passages. If we are interested in the occupation probability, the final time does not matter if it is large enough for applying the adiabatic-impulse model. It is understandable that after the transition (when the energy levels are far from each other) the final time occurs only at the phase.

Appendix B: Adiabatic evolution in the diabatic basis

If we want to prepare the state with some special phase we can use the adiabatic evolution. This evolution is described by the following matrix in the adiabatic basis

$$U_{\text{ad}}(t_f, t_i) = \begin{pmatrix} \exp(-i\zeta) & 0 \\ 0 & \exp(i\zeta) \end{pmatrix}, \quad (\text{B1})$$

where

$$\zeta(t_f, t_i) = \frac{1}{2\hbar} \int_{t_i}^{t_f} \sqrt{\Delta^2 + \varepsilon(t)^2} dt. \quad (\text{B2})$$

If the drive is constant $\varepsilon(t) = \varepsilon_0$, the evolution is described by

$$U_{\text{ad}}(t_f, t_i) = \begin{pmatrix} \exp[-i\omega t_{\text{wait}}] & 0 \\ 0 & \exp[i\omega t_{\text{wait}}] \end{pmatrix}, \quad (\text{B3})$$

where we introduce the following notation $t_{\text{wait}} = t_f - t_i$ and

$$\omega = \frac{\sqrt{\Delta^2 + \varepsilon_0^2}}{2\hbar}. \quad (\text{B4})$$

The adiabatic and diabatic bases are related in the following way

$$|\varphi_{\pm}\rangle = \gamma_{\mp} |\psi_{-}\rangle \mp \gamma_{\pm} |\psi_{+}\rangle, \quad (\text{B5})$$

where

$$\gamma_{\pm} = \frac{1}{\sqrt{2}} \sqrt{1 \pm \frac{\varepsilon(t)}{\sqrt{\Delta^2 + \varepsilon(t)^2}}}. \quad (\text{B6})$$

The matrix which describes the transition from the diabatic basis to the adiabatic one is

$$\mathcal{M} = \begin{pmatrix} \gamma_{-} & -\gamma_{+} \\ \gamma_{+} & \gamma_{-} \end{pmatrix}. \quad (\text{B7})$$

The matrix \mathcal{M} is unitary, so the adiabatic evolution in the diabatic basis is described by the matrix

$$U_{\text{ad}}^{\text{diab}}(t_f, t_i) = \mathcal{M}^T U_{\text{ad}}(t_f, t_i) \mathcal{M}, \quad (\text{B8})$$

$$U_{\text{ad}}^{\text{diab}}(t_f, t_i) = \begin{pmatrix} \gamma_-^2 e^{-i\omega t_{\text{wait}}} + \gamma_+^2 e^{i\omega t_{\text{wait}}} & \gamma_- \gamma_+ (\exp[i\omega t_{\text{wait}}] - \exp[-i\omega t_{\text{wait}}]) \\ \gamma_- \gamma_+ (\exp[i\omega t_{\text{wait}}] - \exp[-i\omega t_{\text{wait}}]) & \gamma_+^2 \exp[-i\omega t_{\text{wait}}] + \gamma_-^2 \exp[i\omega t_{\text{wait}}] \end{pmatrix}. \quad (\text{B9})$$

The same result could be obtained by directly solving the Schrödinger equation in the diabatic basis.

If the adiabatic evolution is far from the crossing energy levels region, $|\varepsilon_0| \gg \Delta$, the adiabatic evolution will be

$$\varepsilon_0 < 0 : U_{\text{ad}}^{\text{diab}}(t_f, t_i) = \begin{pmatrix} \exp[-i\omega t_{\text{wait}}] & 0 \\ 0 & \exp[i\omega t_{\text{wait}}] \end{pmatrix}; \quad (\text{B10})$$

$$\varepsilon_0 > 0 : U_{\text{ad}}^{\text{diab}}(t_f, t_i) = \begin{pmatrix} \exp[i\omega t_{\text{wait}}] & 0 \\ 0 & \exp[-i\omega t_{\text{wait}}] \end{pmatrix}. \quad (\text{B11})$$

It shows that (for the different signs of ε_0) the rotations along the z axis are in different directions, and the visualization is presented in Fig. 5.

Appendix C: Adiabatic basis

The matrix which describes the transition from a diabatic basis to the adiabatic one is Eq. (B7). Using this relation and assuming that we are far from the quasi-crossing region, we obtain the transition matrix in the adiabatic basis

$$\tilde{N}^{\text{ad}} = \begin{pmatrix} (\sqrt{T})^* e^{-2i\zeta(\tau_a)} & -\sqrt{R} \\ \sqrt{R} & \sqrt{T} e^{2i\zeta(\tau_a)} \end{pmatrix}. \quad (\text{C1})$$

The wave function in the adiabatic basis is

$$\varphi = \begin{pmatrix} b_1 \\ b_2 \end{pmatrix}. \quad (\text{C2})$$

Then if b_{1i} and b_{2i} are the initial components of the spinor, the final components become

$$b_{1f} = \sqrt{1 - \mathcal{P}} \exp[-i(2\zeta(\tau_a) + \varphi_S)] b_{1i} - \sqrt{\mathcal{P}} b_{2i}, \quad (\text{C3})$$

$$b_{2f} = \sqrt{\mathcal{P}} b_{1i} + \sqrt{1 - \mathcal{P}} \exp[i(2\zeta(\tau_a) + \varphi_S)] b_{2i}. \quad (\text{C4})$$

Then the occupation probability becomes

$$P_+ = |b_{1f}|^2 = (1 - \mathcal{P}) b_{1i}^2 + \mathcal{P} b_{2i}^2 + 2\sqrt{\mathcal{P}(1 - \mathcal{P})} b_{1i} b_{2i} \cos \theta, \quad (\text{C5})$$

where θ is defined in Eq. (20) and the initial components of the spinor satisfy the following relation $b_{2i} = \sqrt{1 - b_{1i}^2} e^{i\phi_i}$.

The condition for staying in the same state as the initial one after the transition is given by

$$\cos \theta = \frac{(2b_{1i}^2 - 1) \sqrt{\mathcal{P}}}{2b_{1i} \sqrt{1 - b_{1i}^2} \sqrt{1 - \mathcal{P}}}. \quad (\text{C6})$$

The condition of the existence of $\cos \theta$ becomes

$$\delta > \delta_{\text{st}}^{\text{ad}} = -\frac{1}{2\pi} \ln [4b_{1i}^2(1 - b_{1i}^2)]. \quad (\text{C7})$$

Appendix D: Generalization of the problem

If we consider a non-linear perturbation which could be described by the adiabatic-impulse model, then all the above formulas could be generalized. According to the adiabatic-impulse model, the dynamics will be separated on three stages: adiabatic

$$U_{\text{ad}} = \begin{pmatrix} \exp(-i\zeta_1) & 0 \\ 0 & \exp(i\zeta_1) \end{pmatrix}; \quad (\text{D1})$$

transition

$$N = \begin{pmatrix} N_{11} & N_{12} \\ N_{21} & N_{22} \end{pmatrix}; \quad (\text{D2})$$

and adiabatic again

$$U_{\text{ad}} = \begin{pmatrix} \exp(i\zeta_2) & 0 \\ 0 & \exp(-i\zeta_2) \end{pmatrix}, \quad (\text{D3})$$

where ζ is defined in Eq. (B2). The initial state is the same as Eq. (15). Then the components of the wave function are

$$\alpha_f = N_{11} \alpha_i \exp[i(\zeta_2 - \zeta_1)] + N_{12} \beta_i \exp[i(\zeta_1 + \zeta_2)], \quad (\text{D4})$$

$$\beta_f = N_{21} \alpha_i \exp[-i(\zeta_1 + \zeta_2)] + N_{22} \beta_i \exp[i(\zeta_1 - \zeta_2)]. \quad (\text{D5})$$

Then the occupation probability of $|0\rangle$ becomes

$$|\alpha_f|^2 = |N_{11}|^2 \alpha_i^2 + |N_{12}|^2 (1 - \alpha_i^2)$$

$$+ 2\alpha_i \sqrt{1 - \alpha_i^2} |N_{11}| |N_{12}| \cos(2\zeta_1 + \phi_i + \varphi_{11} - \varphi_{12}), \quad (\text{D6})$$

where the components of the transfer matrix are rewritten as $N_{11} = |N_{11}| e^{i\varphi_{11}}$ and $N_{12} = |N_{12}| e^{i\varphi_{12}}$. As a result, we see that all the dependence on phase is in the cosine at the one term which is associated with interference. It shows that all results are applicable not only for the linear perturbation but also for any perturbation which could be approximated by adiabatic-impulse model [44].

In Fig. 6 we show the dependencies of the constructive and destructive interference on time for different initial occupation probabilities and different adiabaticity parameters.

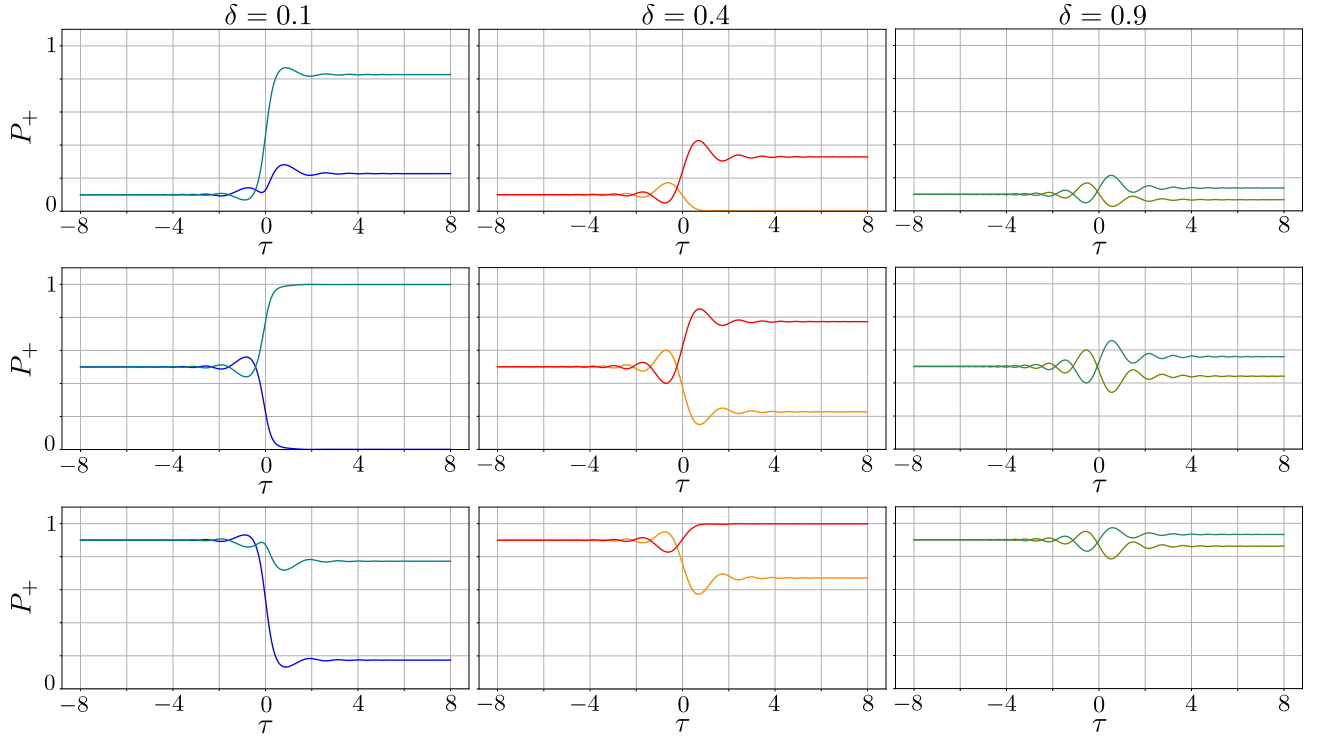


FIG. 6. Dependence of the constructive/destructive interference on the adiabaticity parameter δ for different initial occupation probability in the diabatic basis. The three columns correspond to three adiabaticity parameters δ . Each panel shows the dynamics of the occupation probability \mathcal{P}_+ versus the dimensionless time τ . These dynamical evolutions show that the impact of the interference is smaller when δ is larger. Maximal width is when the initial occupation probability is equal to 0.5 (see the second row)

-
- [1] A. Emmanouilidou, X.-G. Zhao, P. Ao, and Q. Niu, “Steering an eigenstate to a destination,” *Phys. Rev. Lett.* **85**, 1626 (2000).
 - [2] L. Childress and J. McIntyre, “Multifrequency spin resonance in diamond,” *Phys. Rev. A* **82**, 033839 (2010).
 - [3] M. G. Bason, M. Viteau, N. Malossi, P. Huillery, E. Arimondo, D. Ciampini, R. Fazio, V. Giovannetti, R. Mannella, and O. Morsch, “High-fidelity quantum driving,” *Nat. Phys.* **8**, 147 (2012).
 - [4] D. Gagnon, F. Fillion-Gourdeau, J. Dumont, C. Lefebvre, and S. MacLean, “Suppression of multiphoton resonances in driven quantum systems via pulse shape optimization,” *Phys. Rev. Lett.* **119**, 053203 (2017).
 - [5] Z.-Y. Wang and M. B. Plenio, “Necessary and sufficient condition for quantum adiabatic evolution by unitary control fields,” *Phys. Rev. A* **93**, 052107 (2016).
 - [6] R. D. Wilson, A. M. Zagoskin, S. Savel'ev, M. J. Everitt, and F. Nori, “Feedback-controlled adiabatic quantum computation,” *Phys. Rev. A* **86**, 052306 (2012).
 - [7] Y.-x. Liu, J. Q. You, L. F. Wei, C. P. Sun, and F. Nori, “Optical selection rules and phase-dependent adiabatic state control in a superconducting quantum circuit,” *Phys. Rev. Lett.* **95**, 087001 (2005).
 - [8] S. Ashhab, J. R. Johansson, and F. Nori, “Decoherence in a scalable adiabatic quantum computer,” *Phys. Rev. A* **74**, 052330 (2006).
 - [9] D. L. Campbell, Y.-P. Shim, B. Kannan, R. Winik, D. K. Kim, A. Melville, B. M. Niedzielski, J. L. Yoder, C. Tahan, S. Gustavsson, and W. D. Oliver, “Universal nonadiabatic control of small-gap superconducting qubits,” *Phys. Rev. X* **10**, 041051 (2020).
 - [10] A. M. Zagoskin, *Quantum Engineering* (Cambridge University Press, 2011).
 - [11] Y. Atia, Y. Oren, and N. Katz, “Robust diabatic Grover search by Landau-Zener-Stückelberg oscillations,” *Entropy* **21**, 937 (2019).
 - [12] F. Grossmann, P. Jung, T. Dittrich, and P. Hänggi, “Tunneling in a periodically driven bistable system,” *Zeitschrift für Physik B Condensed Matter* **84**, 315 (1991).
 - [13] F. Grossmann, T. Dittrich, P. Jung, and P. Hänggi, “Coherent destruction of tunneling,” *Phys. Rev. Lett.* **67**, 516 (1991).
 - [14] M. Grifoni and P. Hänggi, “Driven quantum tunneling,” *Phys. Rep.* **304**, 229 (1998).
 - [15] M. Wubs, “Instantaneous coherent destruction of tunneling and fast quantum state preparation for strongly pulsed spin qubits in diamond,” *Chem. Phys.* **375**, 163 (2010).
 - [16] Q. Miao and Y. Zheng, “Coherent destruction of tunnel-

- ing in two-level system driven across avoided crossing via photon statistics,” *Sci. Rep.* **6**, 28959 (2016).
- [17] F. Großmann and P. Hänggi, “Localization in a driven two-level dynamics,” *EPL* **18**, 571 (1992).
- [18] J. M. G. Llorente and J. Plata, “Tunneling control in a two-level system,” *Phys. Rev. A* **45**, R6958 (1992).
- [19] Y. Kayanuma, “Role of phase coherence in the transition dynamics of a periodically driven two-level system,” *Phys. Rev. A* **50**, 843 (1994).
- [20] Y. Kayanuma and K. Saito, “Coherent destruction of tunneling, dynamic localization, and the Landau-Zener formula,” *Phys. Rev. A* **77**, 010101 (2008).
- [21] S. Ashhab, J. R. Johansson, A. M. Zagorin, and F. Nori, “Two-level systems driven by large-amplitude fields,” *Phys. Rev. A* **75**, 063414 (2007).
- [22] X. Hu, S. Sun, and Y. Zheng, “Witnessing localization of a quantum state via quantum speed limits in a driven avoided-level crossing system,” *J. Chem. Phys.* **156**, 134113 (2022).
- [23] M. V. Berry, “Transitionless quantum driving,” *J. Phys. A: Math. Theor.* **42**, 365303 (2009).
- [24] S. N. Shevchenko, S. Ashhab, and F. Nori, “Landau-Zener-Stückelberg interferometry,” *Phys. Rep.* **492**, 1 (2010).
- [25] O. V. Ivakhnenko, S. N. Shevchenko, and F. Nori, “Nonadiabatic Landau-Zener-Stückelberg-Majorana transitions, dynamics, and interference,” *Phys. Rep.* **995**, 1 (2023).
- [26] E. P. Glasbrenner and W. P. Schleich, “The Landau-Zener formula made simple,” *Journal of Physics B: Atomic, Molecular and Optical Physics* **56**, 104001 (2023).
- [27] K. Fujikawa and H. Suzuki, “Duality in potential curve crossing: Application to quantum coherence,” *Phys. Rev. A* **56**, 3436 (1997).
- [28] P. Carenza and M. D. Marsh, “On the applicability of the Landau-Zener formula to axion-photon conversion,” *J. Cosmol. Astropart. Phys.* **2023**, 021 (2023).
- [29] X. Wang, H. D. Liu, and L. B. Fu, “Nonlinear non-hermitian Landau-Zener-Stückelberg-Majorana interferometry,” *New J. Phys.* **25**, 043032 (2023).
- [30] K. Ono, S. Shevchenko, T. Mori, S. Moriyama, and F. Nori, “Quantum interferometry with a g -factor-tunable spin qubit,” *Phys. Rev. Lett.* **122**, 207703 (2019).
- [31] P. Y. Wen, O. V. Ivakhnenko, M. A. Nakonechnyi, B. Suri, J.-J. Lin, W.-J. Lin, J. C. Chen, S. N. Shevchenko, F. Nori, and I.-C. Hoi, “Landau-Zener-Stückelberg-Majorana interferometry of a superconducting qubit in front of a mirror,” *Phys. Rev. B* **102**, 075448 (2020).
- [32] M. P. Liul, C.-H. Chien, C.-Y. Chen, P. Y. Wen, J. C. Chen, Y.-H. Lin, S. N. Shevchenko, F. Nori, and I.-C. Hoi, “Coherent dynamics of a photon-dressed qubit,” *Phys. Rev. B* **107**, 195441 (2023).
- [33] A. Paila, J. Tuorila, M. Sillanpää, D. Gunnarsson, J. Sarkar, Y. Makhlin, E. Thuneberg, and P. Hakonen, “Interband transitions and interference effects in superconducting qubits,” *Quantum Inf. Process.* **8**, 245 (2009).
- [34] M. Sillanpää, T. Lehtinen, A. Paila, Y. Makhlin, and P. Hakonen, “Continuous-time monitoring of Landau-Zener interference in a Cooper-pair box,” *Phys. Rev. Lett.* **96**, 187002 (2006).
- [35] W. D. Oliver, Y. Yu, J. C. Lee, K. K. Berggren, L. S. Levitov, and T. P. Orlando, “Mach-Zehnder interferometry in a strongly driven superconducting qubit,” *Science* **310**, 1653 (2005).
- [36] W. D. Oliver and S. O. Valenzuela, “Large-amplitude driving of a superconducting artificial atom,” *Quantum Inf. Process.* **8**, 261 (2009).
- [37] Y. Cao and T. F. Xu, “Nonlinear Landau-Zener tunneling under higher-order dispersion,” *Phys. Rev. A* **107**, 032420 (2023).
- [38] Z. He, K. Titimbo, D. C. Garrett, S. S. Kahraman, and L. V. Wang, “Numerical modeling of the multi-stage Stern-Gerlach experiment by Frisch and Segrè using co-quantum dynamics via the Schrödinger equation,” (2023), [arXiv:2208.14588 \[quant-ph\]](https://arxiv.org/abs/2208.14588).
- [39] C. Heide, T. Boolakee, T. Higuchi, and P. Hommelhoff, “Adiabaticity parameters for the categorization of light-matter interaction: From weak to strong driving,” *Phys. Rev. A* **104**, 023103 (2021).
- [40] C. Heide, T. Boolakee, T. Higuchi, and P. Hommelhoff, “Sub-cycle temporal evolution of light-induced electron dynamics in hexagonal 2D materials,” *J. Phys. Phot.* **2**, 024004 (2020).
- [41] C. Heide, T. Boolakee, T. Higuchi, H. B. Weber, and P. Hommelhoff, “Interaction of carrier envelope phase-stable laser pulses with graphene: the transition from the weak-field to the strong-field regime,” *New J. Phys.* **21**, 045003 (2019).
- [42] T. Higuchi, C. Heide, K. Ullmann, H. B. Weber, and P. Hommelhoff, “Light-field-driven currents in graphene,” *Nature* **550**, 224 (2017).
- [43] M. Wubs, K. Saito, S. Kohler, Y. Kayanuma, and P. Hänggi, “Landau-Zener transitions in qubits controlled by electromagnetic fields,” *New J. Phys.* **7**, 218 (2005).
- [44] P. O. Kofman, O. V. Ivakhnenko, S. N. Shevchenko, and F. Nori, “Majorana’s approach to nonadiabatic transitions validates the adiabatic-impulse approximation,” *Sci. Rep.* **13**, 5053 (2023).
- [45] M. V. Moskalets, *Scattering matrix approach to non-stationary quantum transport* (World Scientific Pub Co Inc, Singapore, 2011).